Design of Class-E Power Amplifier With Nonlinear Components by Using Extended Impedance Method

Junrui Liang
School of Informaiton Science and Technology, ShanghaiTech University
No. 100 Haike Road, Pudong, Shanghai 201210, China
Email: liangjr@shanghaitech.edu.cn

***Abstract*—It has been shown in the previous study that the class-E power amplifier (PA) circuit can be efficiently simulated and optimized in the frequency domain by modeling the whole circuit with the extended impedance method (EIM). This paper reports a breakthrough in the EIM based class-E PA design by taking the nonlinear components into consideration. In analysis, the effect of the two state-dependent nonlinear components in a practical MOSFET switch, i.e., the parasitic drain-to-source junction capacitance and the body diode, is turned into the time-dependent characteristics by carrying out the states-to-time mapping. Iterative computation is necessary for obtaining the steady-state waveforms in view of the nonlinear components. Yet, given the high efficiency of EIM, it is proved that the EIM based optimization runs much faster than the state-of-the-art numerical class-E PA optimization.**

I. Introduction

Power amplifier (PA) is an essential building block in modern communication systems [1]. Among the different classes of PAs, the switch-mode class-E PA has high conversion efficiency at high frequency [2]–[5]. Nowadays, most semiconductor switches used in class-E PAs are MOSFET, whose actual behavior is more complex than an ideal switch. In particular there are some nonlinear components in a MOSFET, such as the body diode [6] and the parasitic drain-to-source junction capacitance [7]–[9]. In addition, the effect of the junction capacitance increases as the operating frequency increases [8]. Therefore, these nonlinearities should receive sufficient consideration towards the optimal design of class-E PA.

The emergence of class-E PA began from the zero voltage switching (ZVS) and zero derivative switching (ZDS) conceptual waveforms and the single-ended implementation with only six circuit components, in which many parameters were assumed ideal or preset [2]. More practical parameters and issues have received consideration in later analyses [7]–[9]. Up to now, most of the studies on class-E PA were carried out analytically in the time domain [3], [7]–[10]. On the other hand, some computational methods were also developed for the numerical simulation and optimization of class-E circuits. These methods are generally based on time-domain state-space technique [4], [6], [11], [12] or frequency-domain simulation [13], [14]. In particular, frequency-domain methods are good at steady-state simulation of power circuits [15], [16].

One of the efficient frequency-domain simulation scheme is called the *extended impedance method* (EIM) [14]. In the class-E analysis using EIM, the switch device is modeled as a time-varying resistance, whose impedance can be expressed in matrix form (after the conceptual extension). Therefore, class-E circuit without nonlinear components can be simulated by applying the basic circuit laws. This paper introduces a breakthrough of EIM by extending its usage to class-E circuit with nonlinear components.

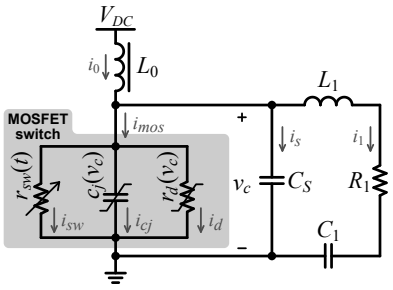

Fig. 1. Class-E PA with practical MOSFET model.

II. EIM based Class-E PA Analysis [14]

As illustrated in Fig. 1, a single-ended class-E PA is composed of six basic components, the chock inductor L_0, switch device (MOSFET), shunt capacitor C_S, and the three L_1, C_1, R_1, which form the resonant network. Considering the periodic triggering and parasitic nonlinearities, a MOSFET can be further broken down into three detailed sub-components: the time-varying resistor r_{sw} [14], the parasitic nonlinear drain-to-source junction capacitor c_j [8], and the nonlinear resistor r_d representing the body diode [6]. The value of r_{sw} periodically changes with respect to time. It induces the power conversion from the dc supply to ac output. The EIM achieves efficient frequency-domain simulation by modeling the time-varying r_{sw} into an impedance in matrix form.

In the time domain, we can have the constitutive relation of r_{sw} as follows

$$v_S(t) = r_{sw}(t)\ i_S(t)\,, \tag{1}$$

where $v_S(t)$ denotes the voltage across r_{sw} and $i_S(t)$ denotes the current flowing through r_{sw}. Since time-domain multiplication corresponds to frequency-domain convolution, in the frequency domain, the relation given by (1) can be derived into

$$V_S(j\omega) = R_{sw}(j\omega) * I_S(j\omega)\,. \tag{2}$$

978-1-4799-5341-7/16/$31.00 ©2016 IEEE

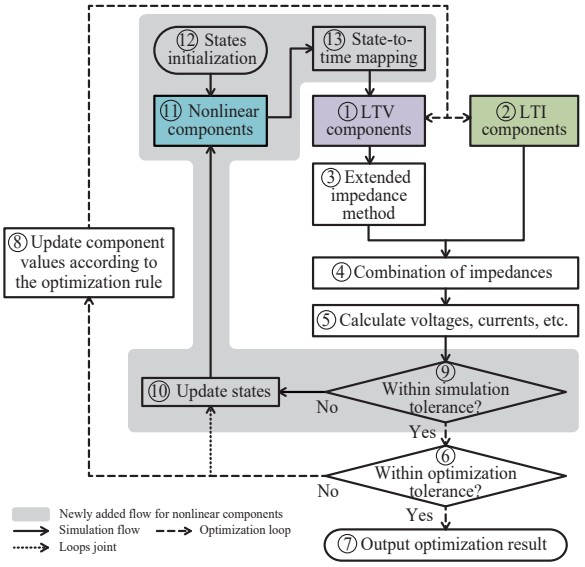

Fig. 2. Flow chart for the EIM based class-E PA design processes.

Expended (2) into truncated vector and matrix form, we have

$$\mathbf{V_S} = \mathbf{Z_{sw}}\,\mathbf{I_S}\,, \tag{3}$$

where $\mathbf{V_S}$ and $\mathbf{I_S}$ are $(2K+1)\times 1$ vectors composed of the Fourier series of v_S and i_S, respectively. The $(2K+1)\times(2K+1)$ matrix $\mathbf{Z_{sw}}$ is defined as the *impedance of the time-varying resistance* r_{sw}. The impedance matrices of the ordinary circuit components can be obtained as diagonal matrices.

Putting aside the parasitic nonlinearities of the switching device, which is a reasonable approximation under the nominal ZVS/ZDS condition and low-frequency operation, the class-E circuit can be formulated as a combination of the six impedances

$$\mathbf{Z_{Class-E}} = \mathbf{Z_{L0}} + [\mathbf{Z_{sw}}\|\mathbf{Z_{Cs}}\|(\mathbf{Z_{L1}} + \mathbf{Z_{C1}} + \mathbf{Z_R})]\,, \tag{4}$$

where "‖" means parallel connection.

By extending the concept of impedance, the voltage and current in the class-E circuit without nonlinear components can be solved with the conventional circuit laws. For example, the vector form of the characteristic voltage v_C (denoted in Fig. 1) can be obtained as follows

$$\mathbf{V_C} = [\mathbf{Z_{Class-E}} - \mathbf{Z_{L0}}]\,\mathbf{Z^{-1}_{Class-E}}\mathbf{V_{DC}}\,, \tag{5}$$

where $\mathbf{V_{DC}}$ is the corresponding vector of the dc supply V_{DC}. Time-domain waveforms can be obtained by doing Fourier series expansion. The input and output powers as well as the conversion efficiency can be efficiently calculated as well.

The simulation and optimization flow chart is shown in Fig. 2 (the highlighted part is for the following section). The simulation with LTV components uses blocks ①–⑤. It is a loop-free process. The parameters optimization can be achieved with a single-loop numerical optimization by adding blocks ⑥–⑧, as those achieved in [14].

III. Analysis of Class-E PA with Nonlinear Components

The EIM in the previous study has incorporated the linear time-varying (LTV) components into the scope of impedance. Nevertheless, nowadays, most switch devices used in class-E PA are power MOSFETs, whose parasitic drain-to-source capacitance and body diode are nonlinear. In particular, under high frequency or off-nominal operation, the effect of these components are not negligible. Only when the nonlinear components have been incorporated, the EIM can become a universal tool for class-E PA design.

The value of the drain-to-source junction capacitance in a MOSFET is expressed as follows

$$c_j(v_c) = \begin{cases} C_{j0}\left(1+\dfrac{v_c}{V_{bi}}\right)^{-m}, & v_c \geq 0\,, \\ C_{j0}\,, & v_c < 0\,, \end{cases} \tag{6}$$

where V_{bi} is the built-in potential; v_c is the voltage across the drain and source, as marked in Fig. 1; C_{j0} is the zero-bias junction capacitance, i.e., the capacitance when $v_c = 0$; m is a power typically in the range of 0.3 and 0.4. On the other hand, according to the diode equation, we can model the body diode as a voltage-dependent resistance as follows

$$r_d(v_c) = \begin{cases} \infty\,, & v_c \geq 0\,, \\ \dfrac{-v_c}{I_S\left[e^{-v_c/(nV_T)}-1\right]}, & v_c < 0\,, \end{cases} \tag{7}$$

where I_S is the saturation current; V_D is the forward voltage drop of the diode; V_T is the thermal voltage; n is the ideal factor.

Since both the values of c_j and r_d are functions of v_c, their impedance matrices depend on the circuit states; therefore, cannot be determined before running the circuit. The steady-state problem can be solved by an iterative algorithm. The first round result is calculated by taking the initial v_c as $v_c^{(0)}(t) = 0$, where the number inside the bracket denotes the iterative cycle. Under this assumption, from (6) and (7), we can have the initial conditions as follows

$$c_j^{(0)}(t) = C_{j0}\,, \qquad r_d^{(0)}(t) = \infty\,. \tag{8}$$

The class-E impedance and characteristic voltage in the $(n+1)^{\text{th}}$ cycle can be expressed as follows

$$\mathbf{Z^{(n+1)}_{Class-E}} = \mathbf{Z_{L0}} + \left[\mathbf{Z_{sw}}\|\mathbf{Z^{(n)}_{Cj}}\|\mathbf{Z^{(n)}_{Rd}}\|\mathbf{Z_{Cs}}\|(\mathbf{Z_{L1}} + \mathbf{Z_{C1}} + \mathbf{Z_R})\right], \tag{9}$$

$$\mathbf{V^{(n+1)}_C} = \left[\mathbf{Z^{(n+1)}_{Class-E}} - \mathbf{Z_{L0}}\right]\left[\mathbf{Z^{(n+1)}_{Class-E}}\right]^{-1}\mathbf{V_{DC}}\,. \tag{10}$$

Applying the Fourier expansion, the time-domain expression is obtained as follows

$$v_c^{(n+1)}(t) \approx \left[\, e^{-jK\omega_0 t}\ \cdots\ e^{-j\omega_0 t}\ \ 1\ \ e^{j\omega_0 t}\ \cdots\ e^{jK\omega_0 t}\,\right]\mathbf{V^{(n+1)}_C}, \tag{11}$$

where ω_0 is the fundamental frequency. With $v_c^{(n+1)}(t)$ and according to (6) and (7), the junction capacitance and equivalent conductance of the body diode can be expressed as functions of time in the $(n+1)^{\text{th}}$ cycle, i.e., $c_j^{(n+1)}(t)$ and $g_d^{(n+1)}(t)$. This process is called *state-to-time mapping* in this paper.

The constitutive relation of the time-varying capacitance c_j in time domain is

$$i(t) = c_j(t)\frac{\mathrm{d}v(t)}{\mathrm{d}t}\,. \tag{12}$$

Converting (12) into frequency domain, we can have

$$I(j\omega) = C_j(j\omega) * j\omega V(j\omega)\,. \tag{13}$$

On the other hand, the constitutive relation of the time-varying resistance r_d can be similarly obtained according to (1)–(3). Denoting the k^{th} Fourier coefficient of $c_j^{(n+1)}(t)$ and $r_d^{(n+1)}(t)$ as $C_{j,k}^{(n+1)}$ and $R_{d,k}^{(n+1)}$, respectively, the corresponding impedance matrices can be constructed as follows

$$\mathbf{Z}_{\mathbf{Cj}}^{(n+1)} = \frac{1}{j\omega_0}\begin{bmatrix} -KC_{j,0}^{(n+1)} & \dots & \varepsilon C_{j,-K}^{(n+1)} & \dots & KC_{j,-2K}^{(n+1)} \\ \vdots & \ddots & \ddots & \ddots & \vdots \\ -KC_{j,K}^{(n+1)} & \ddots & \varepsilon C_{j,0}^{(n+1)} & \ddots & KC_{j,-K}^{(n+1)} \\ \vdots & \ddots & \ddots & \ddots & \vdots \\ -KC_{j,2K}^{(n+1)} & \dots & \varepsilon C_{j,K}^{(n+1)} & \dots & KC_{j,0}^{(n+1)} \end{bmatrix}^{-1}, \tag{14}$$

$$\mathbf{Z}_{\mathbf{Rd}}^{(n+1)} = \begin{bmatrix} R_{d,0}^{(n+1)} & \dots & R_{d,-K}^{(n+1)} & \dots & R_{d,-2K}^{(n+1)} \\ \vdots & \ddots & \ddots & \ddots & \vdots \\ R_{d,K}^{(n+1)} & \ddots & R_{d,0}^{(n+1)} & \ddots & R_{d,-K}^{(n+1)} \\ \vdots & \ddots & \ddots & \ddots & \vdots \\ R_{d,2K}^{(n+1)} & \dots & R_{d,K}^{(n+1)} & \dots & R_{d,0}^{(n+1)} \end{bmatrix}. \tag{15}$$

ε in (14) is a small number very close to zero, in order to avoid the matrix singularity. With the updated matrix at the $(n+1)^{\text{th}}$ round of calculation, $\mathbf{V}_{\mathbf{C}}^{(n+2)}$ in the $(n+2)^{\text{th}}$ round can be calculated likewise. The iteration continues until the result satisfies the relative simulation tolerance δ, i.e.,

$$\frac{\left\|\mathbf{V}_{\mathbf{C}}^{(n+1)} - \mathbf{V}_{\mathbf{C}}^{(n)}\right\|}{\left\|\mathbf{V}_{\mathbf{C}}^{(n+1)}\right\|} < \delta\,. \tag{16}$$

Fig. 2 summarizes the simulation and optimization processes for class-E PA with nonlinear components by adding new blocks ⑨–⑬, which are highlighted in gray in Fig. 2.

As the nonlinear components are able to be incorporated in the EIM based analysis, parameters in class-E PA with nonlinearities can also be optimized using the established numerical methods [14]. Since the nonlinear components has introduced one loop to the simulation, there are two nesting loops towards the optimization task. Sekiya et al. [4] combined both simulation and optimization in a single iteration in their time-domain optimization. This idea can also be used here for reducing the computing effort. The loop joint can be added at the state updating step, as illustrated by the dotted arrow in Fig. 2.

IV. Case Study

The classical design equations provided by N. O. Sokal, the inventor of class-E PA, have only considered the linear conditions [17]. Later analytical studies considering the nonlinear components have involved long equations [7]–[9]. Another design philosophy is to make an initial guess by assuming no nonlinear components, and approach the nominal points by using the numerical methods [4], [14]. In this EIM based study, we start from an initial guess, then used the aforementioned efficient formula to optimize the parameters by taking the nonlinearities into consideration.

TABLE I
Parameters of a Class-E PA Circuit

Parameter	Value	Parameter	Value
V_{DC}	24 V	MOSFET	IRF510
f_0	4 MHz	R_{on} (Rd+Rs)	0.47 Ω
D	50 %	R_{off} (Rds)	444.4 kΩ
L_0	45.3 μH	C_{j0} (Cbd)	366.5 pF
C_S	1.83 nF (lin.) 1.83 nF−C_{j0} (nonlin.)	V_{bi} (Pb)	0.8 V
L_1	0.91 μH	m (Mj)	0.5
C_1	2.35 nF	I_S (Is)	202.9 fA
R_1	4.56 Ω	n (N)	1
Q ($\omega_0 L_1/R_1$)	5	V_t	26 mV

The parameters in the first column are generated based on the revised design equations of [17]; those in the third column are extracted from the SPICE level 3 model of the power MOSFET IRF510; the bracketed parameters are the corresponding aliases in SPICE.

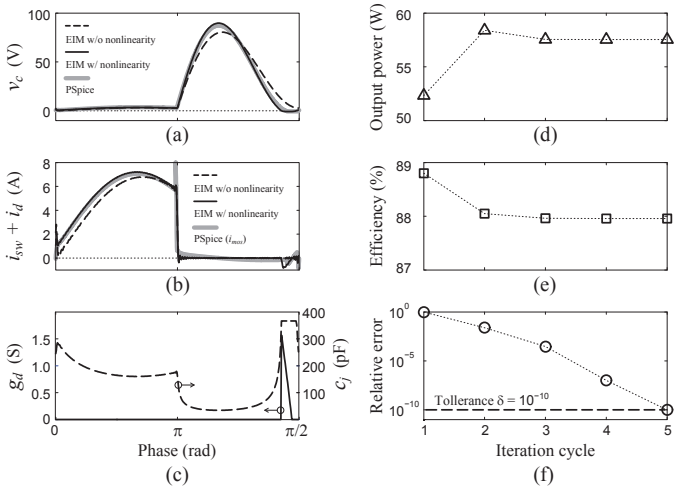

Fig. 3. Simulation result of a class-E PA. (a) switch voltage. (b) swtich current (only i_{mos} can be measured in PSpice because of model encapsulation). (c) Nonlinear conductance ($1/r_d$) and capacitance c_j as functions of time. (d) Convergence of output power. (e) Convergence of conversion efficiency. (f) Relative error in simulation.

The initial parameters are listed in Table I. Circuit parameters are derived by using Sokal's formula [17]. IRF510 is used as the switch device. Its parameters are extracted from the corresponding SPICE model. PSpice simulation is taken as an established reference for the EIM based analysis.

A. Simulation

Simulation is carried out for verifying the EIM based class-E PA analysis with real MOSFET model. The algorithm is implemented with Matlab code. The simulation results, including waveforms, values of nonlinear components, the convergences of output power and conversion efficiency, are

TABLE II
OPTIMIZATION RESULTS OF CLASS-E PA CONSIDERING NONLINEARITIES

	C_S	C_1	Runtime
Double loop	1.7120 pF	2.3979 pF	617.6 ms
Joint loop	1.7131 pF	2.3978 pF	109.2 ms

Optimization is run on a desktop PC equipped with Intel Core i5-4570 CPU @ 3.20 GHz and 8.0 GB RAM; K = 50; Both simulation and optimization tolerances are set to 10^{-10}. The listed running time is an average of 100 cases.

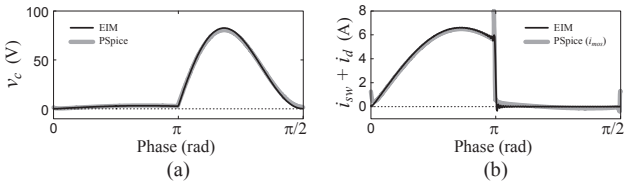

Fig. 4. Waveforms in optimized class-E PA with nonlinear components. (a) switch voltage. (b) swtich current (only i_{mos} can be measured in PSpice because of model encapsulation).

shown in Fig. 3. As it can be observed, this set of parameters gives a nominal operation under linear case (dashed lines in Fig. 3(a) and (b)). Yet, after replacing the ideal switch with a MOSFET model and decreasing C_S by C_{j0}, the nominal operation is violated. Based on the formula introduced in this paper, it is able to provide accurate simulation result using the EIM (solid lines) in view of the MOSFET nonlinearities. The simulated waveforms agree with the SPICE result (gray broad lines). From Fig. 3(d)–(f), the simulation only takes five iterations before arriving at the convergent point, whose relative tolerance is 10^{-10}.

B. Optimization

Given its high efficiency in simulation, the EIM can also facilitate the circuit optimization by incorporating some numerical optimization algorithm. In this case study, we use the Matlab build-in function `fminsearch` for unconstrained optimization. Taking ZVS and ZDS as the optimization objective, the aforementioned off-nominal class-E circuit (because of the ignorance of nonlinearities) is pulled back to nominal by tuning two capacitances C_S and C_1. The optimized parameters are listed in Table II, the waveforms are shown in Fig. 4. Both EIM and PSpice results show that the nominal state is attained after the optimization. The program runtime is also recorded for the nesting double loop and joint loop algorithms, as listed in Table II. It shows that the joint loop optimization only take one sixth of the computational effort, compared to the double loop case. Compared to the numerical class-E PA optimization proposed by Sekiya et al. in 2008, which run on a PC with AMD Athlon CPU @ 2.4 GHz and 2.0 GB RAM [4], the EIM based approach only takes about 1/9000 time to run (some benefit is due to the computer upgrade since 2008).

V. CONCLUSIONS

This paper has introduced a breakthrough in the numerical design of class-E power amplifier (PA) with nonlinear components. It was enabled by extending the application scope of the extended impedance method (EIM) to nonlinear components. Simulation result has proved its credibility in class-E circuit analysis with MOSFET model; optimization result has shown its high efficiency in class-E PA design. In addition, since the EIM based analysis is concise and independent of commercial simulators, it has a big potential to be applied to the design of more other nonlinear power conversion circuits.

ACKNOWLEDGMENT

The work described in this paper was supported by the grants from National Natural Science Foundation of China (Project No. 61401277) and ShanghaiTech University (Project No. F-0203-13-003).

REFERENCES

[1] M. K. Kazimierczuk, *RF Power Amplifier (2nd ed.)*. John Wiley & Sons, 2014.
[2] N. Sokal and A. Sokal, "Class E – A new class of high-efficiency tuned single-ended switching power amplifiers," *IEEE J. Solid-St. Circ.*, vol. 10, no. 3, pp. 168–176, June 1975.
[3] M. Kazimierczuk and K. Puczko, "Exact analysis of class E tuned power amplifier at any Q and switch duty cycle," *IEEE T. Circuits and Syst.*, vol. 34, no. 2, pp. 149–159, Feb. 1987.
[4] H. Sekiya, T. Ezawa, and Y. Tanji, "Design procedure for Class E switching circuits allowing implicit circuit equations," *IEEE T. Circuits-I.*, vol. 55, no. 11, pp. 3688–3696, Dec. 2008.
[5] M. Hayati, A. Lotfi, M. Kazimierczuk, and H. Sekiya, "Performance study of class-e power amplifier with a shunt inductor at subnominal condition," *IEEE Trans. Power Electron.*, vol. 28, no. 8, pp. 3834–3844, 2013.
[6] L. Tan, D. Tan, R. McMahon, and D. Carter, "Fifth-order state-space modeling of class E amplifiers with finite-series inductance and an anti-parallel diode at the switch," *IEEE T. Circuits-I.*, vol. 48, no. 9, pp. 1141–1146, Sept. 2001.
[7] T. Suetsugu and M. Kazimierczuk, "Comparison of class-e amplifier with nonlinear and linear shunt capacitance," *IEEE T. Circuits-I.*, vol. 50, no. 8, pp. 1089–1097, Aug. 2003.
[8] X. Wei, H. Sekiya, S. Kuroiwa, T. Suetsugu, and M. K. Kazimierczuk, "Design of class-e amplifier with mosfet linear gate-to-drain and non-linear drain-to-source capacitances," *IEEE Trans. Circuits Syst. Regul. Pap.*, vol. 58, no. 10, pp. 2556–2565, 2011.
[9] M. Hayati, A. Lotfi, M. K. Kazimierczuk, and H. Sekiya, "Analysis and design of class-e power amplifier with mosfet parasitic linear and nonlinear capacitances at any duty ratio," *IEEE Trans. Power Electron.*, vol. 28, no. 11, pp. 5222–5232, 2013.
[10] T. Yang, J. Liang, C. Zhao, and D. Chen, "Analysis and design of class-E power amplifiers at any duty ratio in frequency domain," *Analog Integr. Circuits Signal Process*, vol. 67, no. 2, pp. 149–156, 2011.
[11] P. Reynaert, K. Mertens, and M. Steyaert, "A state-space behavioral model for CMOS class E power amplifiers," *IEEE Trans. Comput. Aided Des. Integr. Circuits Syst.*, vol. 22, no. 2, pp. 132–138, Feb. 2003.
[12] F. del-Aguila-Lopez, P. Pala-Schonwalder, P. Molina-Gaudo, and A. Mediano-Heredia, "A discrete-time technique for the steady-state analysis of nonlinear Class-E amplifiers," *IEEE T. Circuits-I.*, vol. 54, no. 6, pp. 1358–1366, June 2007.
[13] S. Sivakumar and A. Eroglu, "Analysis of Class-E based RF power amplifiers using harmonic modeling," *IEEE T. Circuits-I.*, vol. 57, no. 1, pp. 299–311, Jan. 2010.
[14] J. Liang and W.-H. Liao, "Steady-state simulation and optimization of class-E power amplifiers with extended impedance method," *IEEE Trans. Circuits Syst. Regul. Pap.*, vol. 58, no. 6, pp. 1433–1445, june 2011.
[15] S. Sanders, J. Noworolski, X. Liu, and G. Verghese, "Generalized averaging method for power conversion circuits," *IEEE Trans. Power Electron.*, vol. 6, no. 2, pp. 251–259, Apr. 1991.
[16] S.-C. Wong and A. Brown, "Analysis, modeling, and simulation of series-parallel resonant converter circuits," *IEEE Trans. Power Electron.*, vol. 10, no. 5, pp. 605–614, Sept. 1995.
[17] N. O. Sokal, "Class-E RF power amplifiers," *QEX*, pp. 9–21, Jan./Feb. 2001.